

# Seismic Fragility Curves for Reinforced Concrete Dual System Buildings: Pearl Tower as Case Study

Sarwar S. Ismael and Faris R. Ahmed

Department of Civil Engineering, Faculty of Engineering, Koya University,  
Koya KOY45, Kurdistan Region – F.R. Iraq

**Abstract**—A seismic fragility curve is a visual representation that illustrates the likelihood of a structure surpassing a particular damage or performance limit state caused by an earthquake with a specific intensity or ground motion level. This curve is typically generated using probabilistic seismic hazard analysis and structural reliability analysis methods. It is based on statistical models that rely on past earthquake data and simulations of future earthquake scenarios to predict the structure or system's behavior under seismic forces. In this study, the seismic performance of 30 stories of 95 m height dual system reinforced concrete buildings located in Erbil is evaluated by analyzing three distinct ground motions. A non-linear platform is used to simulate and analyze data, followed by the generation of seismic inter-story drift fragility curves using Incremental Dynamic Analysis. The buildings' seismic structural performance is assessed based on five different performance levels, including operational phase, immediate occupancy, damage control, life safety, and collapse prevention (CP). Each level is associated with different levels of damage and corresponding degrees of functionality and safety. The fragility curves show that the building has a 50% chance of achieving or exceeding the (CP) level with highly intense ground vibrations with peak ground acceleration = 1.6 g. In addition, these curves can be beneficial in creating future local design codes and provide significant support in evaluating the seismic performance of existing buildings.

**Index Terms**—Dual system, Drift, Fragility curve, Incremental dynamic analysis, Seismic risk assessment, Vulnerability.

## I. INTRODUCTION

Earthquakes are a natural phenomenon that can have catastrophic effects on buildings and human life. When an earthquake occurs, the ground shakes and the building responds to the resulting motion, which can lead to damage or collapse if the building is not properly designed and constructed to resist seismic forces. Building damage is the

main cause of seismic losses from earthquakes, and it is critical to assess the vulnerability of structures to seismic hazards, Fig. 1.

To this end, a key tool used in earthquake engineering is the seismic fragility curve (SFGC) technique. It is a graphical representation of the probability of a structure exceeding a given damage state, such as slight, moderate, extensive, or complete damage, as a function of the intensity of the ground motion. SFGCs are generated by analyzing the dynamic response of a structure to a set of ground motion records with increasing levels of intensity, using analytical models such as pushover or incremental dynamic analysis (IDA).

The output of the analysis is a set of curves that depict the probability of exceeding a damage state as a function of the peak ground acceleration (PGA), velocity, or displacement. These curves are then used to estimate the expected damage and loss for a structure under different levels of seismic hazard. The fragility curves used are unique to each building due to the specific fragility analysis carried out (Hancilar, et al., 2014; Vona, 2014).

SFGCs are extensively used in seismic risk analysis for designing and retrofitting buildings and other structures in seismically active regions. Provide a means of quantifying the risk of damage and collapse for various levels of seismic intensity, helping engineers and building owners to make informed decisions about the appropriate design, and retrofitting measures needed to ensure seismic safety and resilience.

Furthermore, SFGCs can be used to identify the most vulnerable components of a structure, allowing engineers to prioritize retrofitting measures and allocate resources efficiently. They can also be used to evaluate the effectiveness of different retrofitting strategies and to optimize the seismic design of new structures.

The fragility functions for different limit states (LSs) of the building are derived by combining the results of structural analysis with the probability distribution function (PDF) of the engineering demand parameter (EDP) given the intensity measure (IM) that represents the distribution. These functions are cumulative distribution functions expressing the seismic intensity in terms of the IM required to reach particular LS (Baker, et al., 2014).

Typically, one or more threshold capacities of the EDP's (i.e., EDP<sub>c</sub>) are associated with LS, and the fragility

ARO-The Scientific Journal of Koya University  
Vol. XI, No. 1 (2023), Article ID: ARO.11172, 8 pages  
DOI: 10.14500/aro.11172

Received: 23 February 2023; Accepted: 03 June 2023  
Regular research paper; Published: 23 June 2023

Corresponding author's e-mail: sarwar.sadiq@koyauniversity.org  
Copyright © 2023 Sarwar S. Ismael and Faris R. Ahmed. This is an open access article distributed under the Creative Commons Attribution License.



function is the probability of the seismic demand EDP exceeding the capacity EDP<sub>c</sub> given the IM. The process of fragility assessment is computationally intensive, and non-linear dynamic analysis is a feasible method due to recent advancements in computer technology (Jalayer and Cornell, 2009). In addition, various methods for evaluating the distribution of EDP given IM and figuring out fragility functions utilizing non-linear dynamic analysis are discussed in this study. The requirements for performance-based seismic design are also discussed to evaluate structural performance. The degree of damage can be determined by using the maximum interstorey drift ratio (IDR), which is commonly used as the EDP.

Xue, et al., 2008 proposed five performance LSs (operational phase [OP], immediate occupancy [IO], damage control [DC], life safety [LS], and collapse prevention [CP]) with different probabilities of exceedance (0.5%, 1.0%, 1.5%, 2.0%, and 2.5%) to evaluate the building's seismic performance. These LSs are considered when developing fragility curves. Ultimately, SFGCs are crucial for ensuring the safety and resilience of structures in seismically active regions and are a critical tool in earthquake engineering (Xue, et al., 2008; FEMA 273, 1997).

In recent years, many high-rise building been built in Erbil, yet, there are limited amount of researches conducted on the seismic risk assessment of buildings. However, emerging studies have underscored the critical significance of evaluating the vulnerability of pre-seismic code buildings and emergency facilities, emphasizing the pressing need to mitigate their potential seismic losses. These investigations have shed light on the urgency of addressing the seismic resilience of structures in the region, particularly those constructed before the implementation of modern seismic design codes. By recognizing the inherent vulnerability of these buildings and facilities, researchers have highlighted the importance of comprehensive risk assessment methodologies to identify potential weaknesses, assess their performance under seismic loading, and propose effective strategies for minimizing the associated risks (Liel, et al., 2009; Abduljaleel, 2021). The findings of such research can provide crucial insights for policymakers, engineers, and stakeholders involved in enhancing the seismic resilience of the built environment in the city and similar contexts.

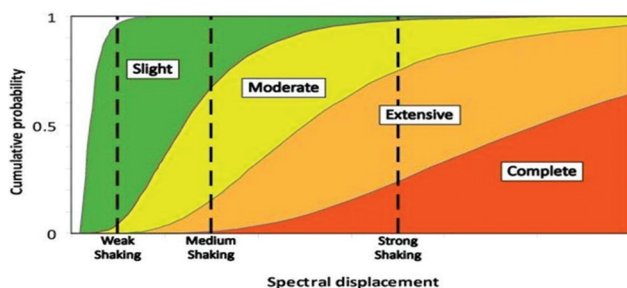


Fig. 1. Fragility curves for different limit states.

## II. METHODOLOGY

Determining fragility required a thorough evaluation of structural response at various intensities. Nonlinear dynamic studies carried out in a variety of ways, with the primary differences being in the post-processing methods and the ground motion selection and scaling techniques that can be used. According to (Vamvatsikos and Cornell, 2004; Jalayer and Cornell, 2009), there are three primary methods for analyzing seismic performance: cloud analysis, stripe analysis, and IDA. Among these, cloud analysis is the least restrictive, as evidenced by the characteristic cloud pattern that emerges in the IM versus EDP plot, with each point representing a single analysis, as shown in Fig. 2 which shows an illustration of the findings from incremental dynamic analyses, which were utilized to determine the (IM) values linked with structural collapse for each of the ground motions.

The process of determining the fragility of a building, which is the likelihood that it will experience structural damage or collapse when subjected to seismic ground motions. To assess the building's performance under seismic loads, IDA technique is used. This technique is considered essential tool for determining a structure's safety margins.

The study develops fragility curves using a probabilistic approach based on five performance levels that are recommended for assessing building performance under seismic loads. These performance levels are defined by the IDR of the building, which is a widely used EDP that is used to assess the degree of damage in a building due to seismic loads. The maximum IDR is considered an excellent indicator for determining the degree of damage (Vamvatsikos and Cornell, 2002).

To generate the fragility curves, various scaling and record set selection strategies can be used. One option is to use a fixed record set that has been scaled to different levels of intensity, typically by multiplying all natural accelerograms by the same scale factor. Alternately, a distinct collection of natural records can be used for each level of IM, and scaling may be completely avoided. Fragility curves are the product

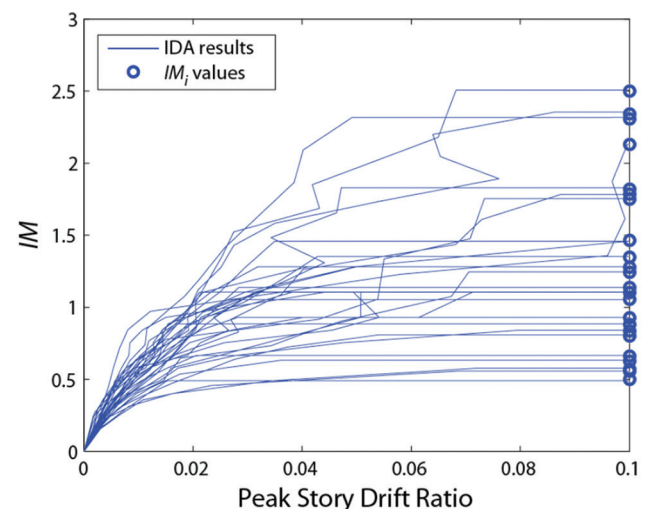


Fig. 2. Illustration of the findings from incremental dynamic analyses.

of seismic fragility analysis which clarify the probability of seismic demand (EDP) exceeding a certain LS at a specific ground motion IM as depicted in equation (1).

$$\text{Fragility} = P(\text{EDP} > \text{LS}/\text{IM}) \quad (1)$$

The fragility information can be extracted in several ways, such as using linear regression in logarithmic space to independently fit the non-collapsing IM-EDP points or using parametric or non-parametric regression (Ibrahim and El-Shami, 2011). Any statistical measure of EDP provided by the IM, such as the mean, 16/50/84 percentile, standard deviation, without the use of parametric or non-parametric regression, may be calculated directly from the relevant EDP data, greatly simplifying post-processing.

Also there are the different methods of analyzing seismic performance, which include cloud analysis, stripe analysis, and IDA. Cloud analysis is the least restrictive, and it produces a characteristic cloud pattern that emerges in the IM versus EDP plot, with each point representing a single analysis. Stripe analysis, on the other hand, uses any number of record sets, similar to cloud analysis, and it must use at least some scaling to ensure that all runs at a particular IM level truly exactly match the IM level requested, without any tolerance. The empirical distribution of the EDP findings taken from the relevant analyses directly represents the distribution of EDP given IM at each IM level. The sole basis for IDA is scaling. It focuses on individual recordings, which are scaled to various intensities until collapse is generally attained.

The decision to use any of the aforementioned methods ultimately rests on the analyst and their comprehension of the issue at hand. If other sources of uncertainty, such as the unpredictability of model parameters, must be taken into account, then more sophisticated (and complex) strategies should be used. Furthermore, the collapse margin ratio, which is recommended as a novel and effective seismic indicator by reference to the FEMA-P-695 methodology, is ultimately determined in this study based on the fragility search technique received from the (IDA). The methodological work for the case study is explained and summarized in the flow chart in Fig. 3.

### A. Earthquake Records

The selection of ground motion recordings is an essential component of developing fragility curves. It is important to choose the appropriate ground motion and scale the ground motions correctly when creating the curves. Arbitrarily scaling ground motion to a specific spectral acceleration,  $S_a$ , at a period,  $T$ , may result in overly conservative structural response (Baker, et al., 2014). Ground motion should be

chosen from previously documented earthquake occurrences. Websites such as the Consortium of Organization for Strong Motion Observation System, K-NET, and the Pacific Earthquake Engineering Research NGA database website can be used to select ground motion. Other websites that provide ground motion data include the European Strong Motion database, the French Accelerometric Network, and the Swiss Earthquake Database (Pagani, et al., 2014).

The appropriate amount of ground motion is determined by the application and predicted structural response. Foreshocks are classified as either near-field site or far-field site ground motions, and the site-to-source distance, magnitude, spectral shape throughout the interest period range, and hazard curve at a period,  $T$ , are crucial variables for far-field sites. Near-field site considerations include spectral form and the potential for velocity pulses. Table I and Fig. 4 provide suggestions for selecting ground motion (Haselton, et al., 2012; SCEC, 2012; USGS Earthquake, n.d.).

Figs. 5-7 provide suggestions for scaling ground motion with recordings scaled to the elastic response spectrum. In an effort to align the previous records (Table I) with the building location and site class, SiesmoMatch software (SEISMOSOFT, 2023) used to match the chosen ground motion data in accordance with the intended target response spectrum using 5% damping, short periods spectral acceleration  $S_s = 0.6$  g, and (1 s) period spectral acceleration  $S_1 = 0.2$  g as per Iraqi seismic code 2017.

### B. Simulations Methods

The NDA and time history analysis (THA) simulation methods have their unique advantages and limitations. The choice of simulation method depends on the specific characteristics of the structure, the level of accuracy required, and the available resources. These simulation methods are critical tools for engineers in assessing the seismic vulnerability of structures and developing strategies to enhance their seismic performance. Non-linear static analysis (NSA) has been employed in various studies such as those by Mosalam, et al. (1997), Di Ludovico, et al. (2013), Lee, et al. (2014), and Lee and Moon (2014). Other simulation methods such as non-linear THA (NL THA) have been utilized in studies by Aiswarya and Mohan (2014), Farsangi, et al. (2014), and Wang and Rosowsky (2014). IDA has also been employed in studies by Charalambos, et al. (2014), Raghunandan, et al. (2014), Dolsek (2009), Vamvatsikos and Fragiadakis (2010), and Sudret, et al. (2014).

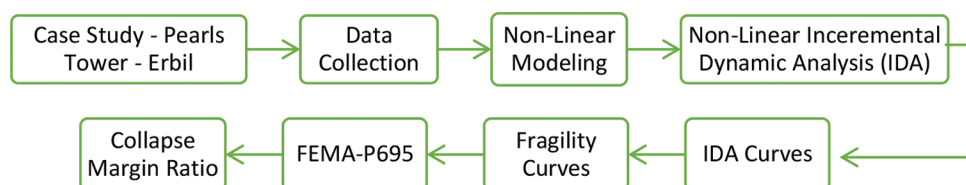


Fig. 3. Outlines and summarizes the methodology of current study.

TABLE I  
GROUND MOTION RECORDS

Description	1940 El Centro earthquake (Imperial Valley-02)*	1995 Great Hanshin earthquake (Kobe Japan)*	1999 İzmit earthquake (Kocaeli, Turkey)*
UTC time	1940 May 19	1995 January 16	1999 August 17
Magnitude, Mw	6.9	7.3	7.6
Duration, s	39.48	20	37
Depth, km	16	17.6	15
Epicenter	32.733N 115.5W	34.59N 135.07E	40.748N 29.864W
Type	Strike-slip	Strike-slip	Strike-slip
Area affected	United State, Mexico	Japan	Turkey
Total damage	\$6 million	\$200 billion	\$3-8.5 billion
Maximum intensity	X (extreme) by Modified Mercalli Scale	XII (extreme) by Modified Mercalli Scale	X (extreme) by Modified Mercalli Scale
Causalities	9 dead 20 injured	6434 dead 43792 injured	18373 dead 48901 injured
PGA (g)	0.281	0.233	0.136

PGA: Peak ground acceleration

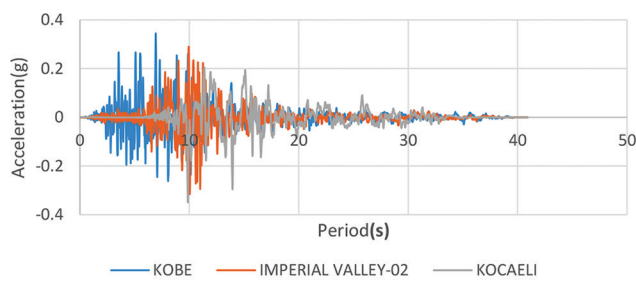


Fig. 4. Acceleration (g) of studied ground motions.

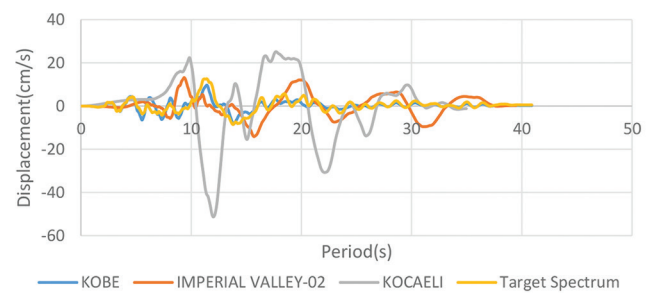


Fig. 7. Displacement (cm/s) of studied ground motions.

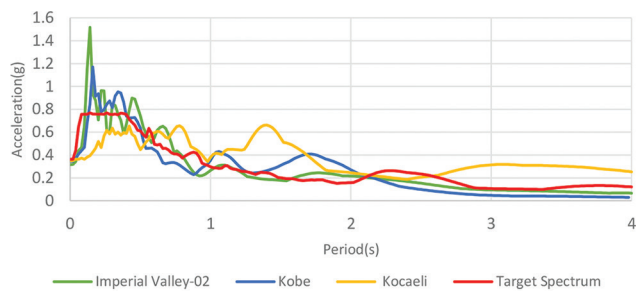


Fig. 5. Fourier transform spectra.

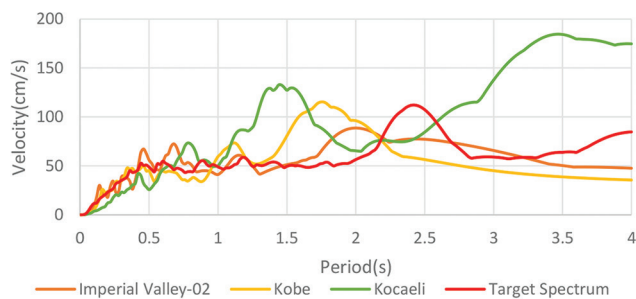


Fig. 6. Velocity (cm/s) of studied ground motions.

#### Non-linear IDA (NL-IDA)

The behavior of a given structure when subjected to seismic excitations of varying intensity, including expected structural response, failures, and losses, is examined through

IDA. The NL-THA (NL-IDA) approach provides more precise outcomes regarding how the structure would react to seismic activity. PGA, also known as PGA, is the most commonly utilized parameter. The relationship between the IDR and the intensity of the ground motion can be leveraged to produce IDA curves, which are referenced in many seismic codes (ASCE, 2016, FEMA 273, 1997) require a minimum of three or seven sets of ground motions. As a result, three sets of powerful ground movements for each model were employed in this work, and they were chosen from the NGA website of the (Berkeley, n.d.). Table II contains statistics on the ground motions which subsequently scaled from 0.1 g to 1.5 g in accordance with the intended target spectrum.

#### SFGC

A fragility curve is a mathematical function that depicts the probability of a structure exceeding a particular level of damage, given a specific ground motion intensity parameter such as PGA or spectral acceleration (SA). The curve provides an estimate of the probability of different levels of damage for a given ground motion intensity and it is often used in seismic risk analysis to evaluate the seismic vulnerability of structures. The maximum roof displacement can be divided by the overall height of the building (92 m) to determine the % drift, as specified in Eq. (1).

$$\% \text{ Drift} = \frac{\text{Roof displacement}}{\text{Building height}} \times 100 \quad (2)$$

The probability of damage ( $P [D/PGA]$ ) is represented as a function of the logarithm of the ground motion intensity parameter (PGA), with mean ( $\mu$ ) and standard deviation ( $\Phi$ ) parameters determining the shape of the curve. The fragility curve equation can be written as follows:

$$P\left[\frac{D}{PGA}\right] = \Phi \frac{\ln(PGA) - \mu}{\sigma} \times 100 \quad (3)$$

Where:  $\Phi$  is the standard normal cumulative distribution function,  $\sigma$  and  $\mu$  are the mean value and standard deviation of logarithm PGA, and  $D$  is the damage state. The fragility curve is typically plotted on a graph, with the PGA values on the x-axis and the probability of exceeding a certain damage level on the y-axis. Damage levels are often expressed as a percentage of the structure's replacement cost, and several damage levels are typically evaluated, such as 0.5%, 1%, 1.5%, 2%, and 2.5% (Xue, et al., 2008; Ibrahim and El-Shami, 2011).

### III. CASE STUDY

This study examines the Pearls Towers project, which is situated on the west side of the Empire World on a 100-m

TABLE II  
SUMMARIZED FLOOR LOADS

Load description	Value
Dead load	
• Finishing	2.5 kPa
• Partition walls	2.0 kPa
• Mechanical, electrical and plumbing	0.5 kPa
Live load	
• Private rooms	1.92 kPa
• Balcony = 1.5*1.92	2.90 kPa
• Corridor	4.79 kPa
• Bathrooms	2.87 kPa
• Staircase	4.79 kPa
• Elevator access	4.79 kPa

road, Erbil, with a total area of 234,000 square meters. The building has a reinforced concrete structure with 30 floors, including 25 residential floors, two commercial floors, and three underground parking floors. The typical floors have an interstorey height of 3.0 m, while the basement and parking levels have a height of 4.0 m, resulting in a total building height of 95 m. The building columns have dimensions of C1 (60 × 170) cm reinforced with 24φ20 + 4φ25 corners, C2 (50 × 150) cm reinforced 24φ20 + φ25 corners, and C3 (70 × 180) cm reinforced 28φ20 + φ25 corners, while the beams are 50 × 55 cm, 50 × 75 cm, and 60 × 55 cm, with a slab thickness of 20 cm as shown in Fig. 8. The concrete has a compressive strength of 50 MPa for the entire structure, while the steel reinforcement has a yield stress of 420 MPa. A 3D model of the structure is created to perform structural analysis, including the effects of seismic and gravity loads, which include dead loads and live loads as shown in Table II per ASCE7-16. The findings are then utilized to establish the performance point of the building through control values.

### IV. RESULTS AND DISCUSSION

#### A. IDA

To evaluate the seismic performance of the structure up to the point of collapse, three different earthquake records used to generate IDA curves as shown in Fig. 9. To do this, it is used NL-THA software to analyze each ground motion and plotted the IDA curves using PGA as the IM and interstorey drift % as the damage measure.

Gradually, it increased the IM of PGA in 0.1 g increments until it reached 1.5 g. At this point, the analysis was stopped due to the structures' dynamic instability. The tower's performance point was evaluated using five performance levels that were represented by vertical gridlines at drifts of 0.5%, 1%, 1.5%, 2%, and 2.5%.

To assess the structure, three cases with different ground motion intensities use as shown in Table I and Figs. 4-7. Refer to Fig. 9 in Case 1 had a strong ground motion intensity of 0.281 g PGA, Case 2 had an intermediate ground

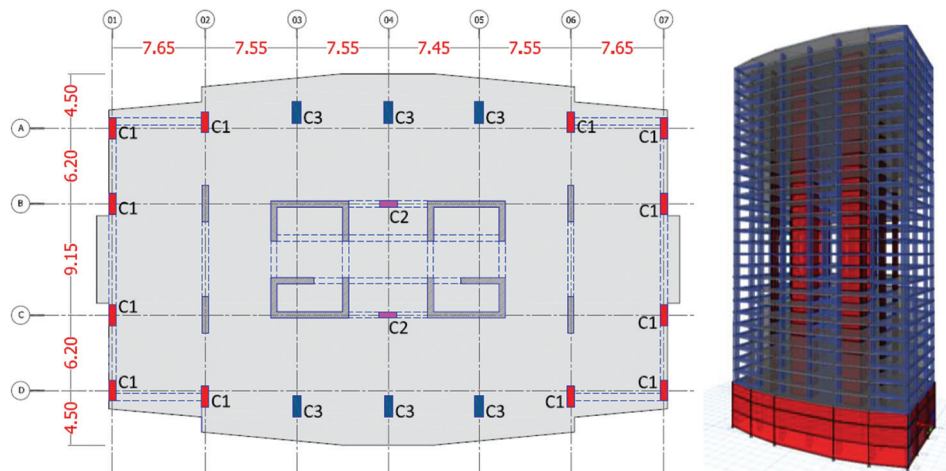


Fig. 8. Plan and isometric view of the building.

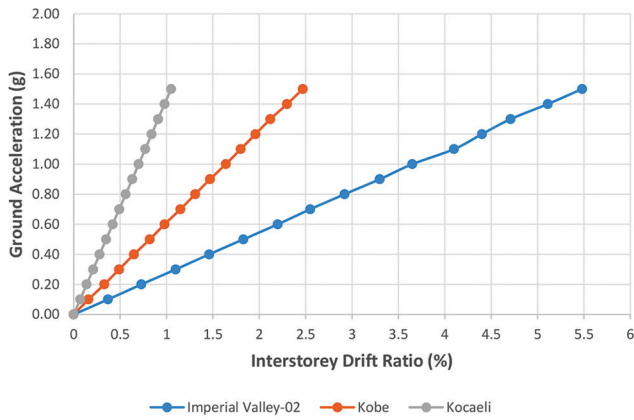


Fig. 9. Incremental dynamic analysis curve for the record data.

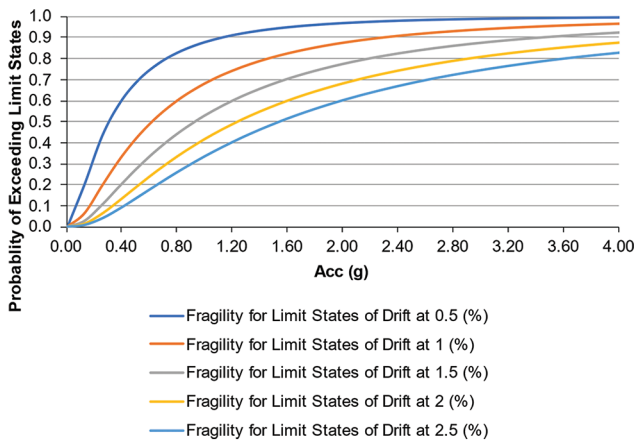


Fig. 10. Seismic fragility curve of the building considering 5 level of damages.

motion intensity of 0.233 g PGA, and Case 3 had a low ground motion intensity of 0.136 g PGA.

The analysis revealed that the building exceeded the DC performance limit of 1.5% and was close to the collapse limit margin for Cases 1 and 2, with IDRs of 1.8% and 1.64%, respectively. In other words, the building would experience significant structural damage in these scenarios.

However, in Case 3, the building was able to maintain its operational performance level during a low-intensity earthquake with an IDR of only 1.0% at a PGA of 1.4 g. This means that the building would experience little to no structural damage and would continue to function normally in this scenario. Overall, the IDA analysis revealed important information about the building’s seismic performance and helped to identify the performance limits of the structure.

*B. SFGC*

Fig. 10 presents that the study illustrates the outcomes of the simulation models used. The purpose of the study was to examine the performance of buildings under varying ground motion conditions. The performance levels considered in this study were IO, DC, and CP.

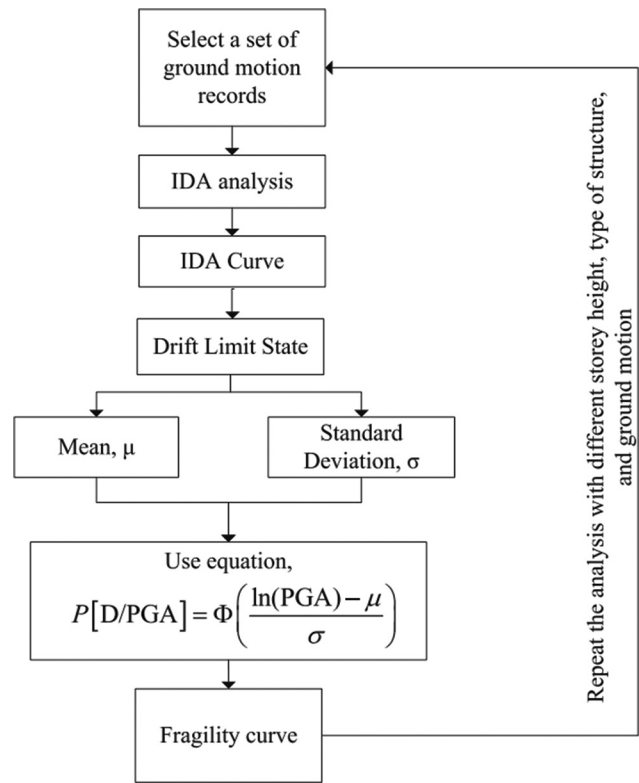


Fig. 11. Flow chart of generating fragility curve.

This study found that the probability of achieving the IO performance level during weak ground vibrations (PGA = 0.2 g) is only 5%. This indicates that the building’s occupants may experience discomfort and some non-structural damage during this level of ground motion.

However, for strong ground motion with PGA > 4.0 g, the probability of reaching or exceeding the IO performance level is 60%. This means that the building can accommodate its occupants with little to no damage during these high-intensity ground vibrations.

In terms of achieving the DC performance level, the study found that for a building equivalent to 1.2 g, the probability of reaching or exceeding the DC performance level is 70%. This suggests that some damage to non-structural elements may occur, but the building’s structural integrity remains intact. In addition, if the building is exposed to PGA = 2.5 g, there is an almost 80% probability of reaching or exceeding the DC performance level.

Furthermore, this study examined the CP performance level, which represents the highest level of performance that a building can achieve. The study found that there is a 60% chance of achieving or exceeding the CP level with highly intense ground vibrations with PGA = 1.6 g. This indicates that both the structural and non-structural components of the building are significantly deteriorating, and the building may be at risk of collapsing.

To summarize, the study provides insights into the performance of buildings under varying ground motion conditions. The fragility curve input and output generated

TABLE III  
THE FRAGILITY CURVE INPUT

Total number of load intensities analyzed	15														
Intensity label	Acc														
Intensity unit	g														
Intensity No.	1	2	3	4	5	6	7	8	9	10	11	12	13	14	15
Acc (g)	0.1	0.2	0.3	0.4	0.5	0.6	0.7	0.8	0.9	1	1.1	1.2	1.3	1.4	1.5
Number of analysis performed in each intensity	3														
Engineering demand parameter (EDP) considered	Drift														
EDP unit	%														
Total number of performance levels considered	5														
Performance level	OP			IO			DC			LS			CP		
Drift limit (%)	0.5		1		1.5		2		2.5						
Acc (g)	Drift (%)				Ln (Drift)										
0.1	0.16				-1.832581										
0.1	0.37				-0.994252										
0.1	0.07				-2.65926										
0.2	0.33				-1.108663										
0.2	0.73				-0.314711										
0.2	0.14				-1.966113										
0.3	0.49				-0.71335										
0.3	1.1				0.09531										
0.3	0.21				-1.560648										
0.4	0.65				-0.430783										
0.4	1.46				0.378436										
0.4	0.28				-1.272966										
0.5	0.82				-0.198451										
0.5	1.83				0.604316										
0.5	0.35				-1.049822										
0.6	0.98				-0.020203										
0.6	2.2				0.788457										
0.6	0.42				-0.867501										
0.7	1.15				0.139762										
0.7	2.55				0.936093										
0.7	0.491				-0.711311										
0.8	1.31				0.270027										
0.8	2.92				1.071584										
0.8	0.561				-0.578034										
0.9	1.47				0.385262										
0.9	3.3				1.193922										
0.9	0.632				-0.458866										
1	1.64				0.494696										
1	3.65				1.294727										
1	0.701				-0.355247										
1.1	1.8				0.587787										
1.1	4.1				1.410987										
1.1	0.771				-0.260067										
1.2	1.96				0.672944										
1.2	4.4				1.481605										
1.2	0.841				-0.173164										
1.3	2.12				0.751416										
1.3	4.71				1.549688										
1.3	0.91				-0.094311										
1.4	2.3				0.832909										
1.4	5.11				1.631199										
1.4	0.98				-0.020203										
1.5	2.47				0.904218										
1.5	5.48				1.701105										
1.5	1.05				0.04879										
Standard deviation	1.4159														
Ln of standard deviation	1.0139														

OP: Operational phase, IO: Immediate occupancy, DC: Damage control, LS: Life safety, and CP: Collapse prevention

TABLE IV  
THE FRAGILITY CURVE OUTPUT

Acc	Fragility for limit states of drift at				
	IO 0.5 (%)	OP 1 (%)	DC 1.5 (%)	LS 2 (%)	CP 2.5 (%)
0.0100	0.03	0	0	0	0
0.1333	20.21	6.45	2.76	1.39	0.77
0.2667	44.05	20.23	10.87	6.46	4.12
0.4000	59.90	33.25	20.25	13.21	9.07
0.5333	70.36	44.08	29.16	20.25	14.62
0.6667	77.49	52.85	37.13	27.02	20.26
0.8000	82.51	59.93	44.10	33.28	25.71
0.9333	86.16	65.68	50.15	38.97	30.85
1.0667	88.86	70.39	55.39	44.11	35.63
1.2000	90.91	74.27	59.94	48.73	40.05
1.3333	92.50	77.51	63.91	52.88	44.12
1.4667	93.74	80.23	67.37	56.60	47.86
1.6000	94.73	82.53	70.40	59.96	51.28
1.7333	95.53	84.49	73.07	62.98	54.43
1.8667	96.18	86.17	75.43	65.71	57.31
2.0000	96.71	87.62	77.53	68.17	59.97
2.1333	97.15	88.88	79.39	70.41	62.41
2.2667	97.52	89.97	81.05	72.45	64.66
2.4000	97.83	90.93	82.55	74.30	66.73
2.5333	98.09	91.77	83.88	75.99	68.65
2.6667	98.32	92.51	85.09	77.54	70.42
2.8000	98.51	93.17	86.18	78.95	72.06
2.9333	98.67	93.75	87.17	80.25	73.59
3.0667	98.82	94.28	88.07	81.45	75.00
3.2000	98.94	94.74	88.88	82.55	76.32
3.3333	99.05	95.16	89.63	83.57	77.54
3.4667	99.14	95.54	90.31	84.51	78.69
3.6000	99.22	95.88	90.93	85.38	79.75
3.7333	99.30	96.18	91.51	86.19	80.75
3.8667	99.36	96.46	92.03	86.94	81.68
4.0000	99.42	96.72	92.52	87.64	82.56

OP: Operational phase, IO: Immediate occupancy, DC: Damage control, LS: Life safety, and CP: Collapse prevention

from the simulation models is presented in the Tables III and IV that provided, which can be used to guide design decisions for buildings in areas with high seismic activity. Fig. 11 illustrates the finding of fragility curve.

### V. CONCLUSION

SFGCs are essential tools for assessing the potential performance of structures under earthquake loading. In this study, the SFGCs were developed for dual system buildings in Erbil city using IDA. The fragility curves were developed for various LSs, including immediate occupancy, life safety, and CP, using the probability of exceedance of a given EDP given the level of an IM. It can be concluded that the building under Weak ground vibrations (PGA = 0.2g) have a low probability (5%) of achieving the maximum performance level, resulting in discomfort and some non-structural damage. Results from IDA show that walls fail at PGA values 5–6 times their design PGA in frame-equivalent systems. Strong ground motion (PGA > 4.0 g) has a higher probability (60%) of meeting the performance level, ensuring minimal damage and occupant safety. For the DC performance level, a building equivalent to

1.2g has a 70% chance of meeting the level, with some non-structural damage but overall structural integrity. Exposure to  $PGA = 2.5g$  increases the probability to nearly 80%.

The CP performance level, representing the highest level, has a 50% chance of being met with  $PGA = 1.6g$ , indicating significant deterioration and collapse risk for both structural and non-structural components. This indicates that the structural components of the building are significantly strong enough to resist up to about 6 times of designed target spectrum. The developed fragility curves are unique to each building due to the specific fragility analysis carried out for each building. The results indicated that the seismic performance objectives of dual system buildings designed according to the current local codes can be achieved with good reliability. The fragility curves developed in this study provide valuable insights for improving the seismic performance of dual system buildings in Erbil city and can serve as a foundation for further research in this area.

#### REFERENCES

- Abduljaleel, Z.A., Taha, B.O., and Yaseen, A.A., 2021. Seismic vulnerability assessment of Rizgary hospital building in Erbil City, the capital city of KR of Iraq. *Journal of Engineering*, 27(8), pp. 59-79.
- Aishwarya, S., and Mohan, N., 2014. Vulnerability analysis by the development of fragility curves. *IOSR Journal of Mechanical and Civil Engineering (IOSR-JMCE)*, 11(2), pp. 33-40.
- ASCE, American Society of Civil Engineering., 2016. *Minimum Design Loads and Associated Criteria for Buildings and Other Structures*. ASCE/SEI, United States.
- Baker, S., Lesaux, N., Jayanthi, M., Dimino, J., Proctor, C.P., Morris, J., Gersten, R., Haymond, K., Kieffer, M.J., and Linan-Thompson, S. 2014. Teaching academic content and literacy to english learners in elementary and middle school. In: *IES Practice Guide, NCEE 2014-4012*. What Works Clearinghouse, United States.
- Berkeley, U.C., n.d. *Ground Motion Selection and Modification (GMSM) Program*. Available from: <https://apps.peer.berkeley.edu/gmsm/home> [Last accessed on 2023 Jun 10].
- Charalambos, G., Dimitrios, V., and Symeon., C., 2014. Damage assessment, cost estimating, and scheduling for post-earthquake building rehabilitation using BIM. In: *Computing in Civil and Building Engineering (2014)*. ASCE, United States, pp. 398-405.
- Di Ludovico, M., Polese, M., d'Aragona, M.G., Prota, A., and Manfredi, G., 2013. A proposal for plastic hinges modification factors for damaged RC columns. *Engineering Structures*, 51, pp. 99-112.
- Dolsek, M., 2009. Incremental dynamic analysis with consideration of modeling uncertainties. *Earthquake Engineering and Structural Dynamics*, 38, 805-825.
- Farsangi, E.N., Rezvani, F.H., Talebi, M., and Hashemi, S.A.H., 2014. Seismic risk analysis of steel-MRFs by means of fragility curves in high seismic zones. *Advances in Structural Engineering*, 17(9), pp. 1227-1240.
- FEMA 273, 1997. *NEHRP Guidelines for the Seismic Rehabilitation of Buildings, prepared by the Building Seismic Safety Council. (FEMA Publication No. 273)*. Federal Emergency Management Agency, Washington, D.C.
- Fragiadakis, M., and Vamvatsikos, D., 2010. Fast performance uncertainty estimation via pushover and approximate IDA. *Earthquake Engineering and Structural Dynamics*, 39(6), pp. 683-703.
- Hancilar, U., Cakti, E., Erdik, M., Franco, G., and Deodatis, G., 2014. Earthquake vulnerability of school buildings: Probabilistic structural fragility analyses. *Soil Dynamics and Earthquake Engineering*, 67, pp. 169-178.
- Haselton, C., Whittaker, A., Hortacsu, A., Baker, J., Bray, J., and Grant, D., 2012. *Selecting and Scaling Earthquake Ground Motions for Performing Response-history Analyses*. In: *Proceedings of the 15th World Conference on Earthquake Engineering, 2012*. Earthquake Engineering Research Institute, Oakland, CA, USA, pp. 4207-4217.
- Ibrahim, Y.E., and El-Shami, M.M., 2011. Seismic fragility curves for mid-rise reinforced concrete frames in Kingdom of Saudi Arabia. *The IES Journal Part A: Civil and Structural Engineering*, 4, pp. 213-223.
- Jalayer, F., and Cornell, C., 2009. Alternative non-linear demand estimation methods for probability-based seismic assessments. *Earthquake Engineering and Structural Dynamics*, 38, pp. 951-972.
- Lee, S.G., Kim, D.H., and Lee, I.K., 2014. Seismic fragility analysis of 5 MW offshore wind turbine. *Renewable Energy*, 65, pp. 250-256.
- Lee, Y.J., and Moon, D.S., 2014. A new methodology of the development of seismic fragility curves. *Smart Structures and Systems*, 14(5), pp. 847-867.
- Liel, A.B., Haselton, C.B., Deierlein, G.G., and Baker, J.W., 2009. Incorporating modeling uncertainties in the assessment of seismic collapse risk of buildings. *Structural Safety*, 31, pp. 197-211.
- Mosalam, K.M., White, R.N., and Gergely, P., 1997. Static response of infilled frames using quasi-static experimentation. *Journal of Structural Engineering*, 123(11), pp. 1462-4169.
- Pagani, M., Monelli, D., Weatherill, G., Danciu, L., Crowley, H., Silva, V., Henshaw, P., Butler, L., Nastasi, M., and Panzeri, L., 2014. OpenQuake engine: An open hazard (and risk) software for the global earthquake model. *Seismological Research Letters*, 85, pp. 692-702.
- Raghunandan, M., Liel, A.B., and Luco, N., 2014. Aftershock collapse vulnerability assessment of reinforced concrete frame structures. *Earthquake Engineering and Structural Dynamics*, 44(3), pp. 419-439.
- SCEC, 2012. *Report on the August 2012, Brawley Earthquake Swarm in Imperial Valley, Southern California*. Southern California Earthquake Center, USA. Available from: <https://www.scec.org/publication/1678> [Last accessed on 2023 Jun 10].
- SEISMOSOFT, 2023. *Earthquake Software for Response Spectrum Matching*. Earthquake Engineering Software Solutions.
- Sudret, B., Mai, C., and Konakli, K., 2014. Assessment of the lognormality assumption of seismic fragility curves using non-parametric representations. arXiv preprint arXiv:1403.5481.
- USGS Earthquake, n.d. *Earthquakes: U.S. Geological Survey*. Available from: <https://www.usgs.gov/programs/earthquake-hazards/earthquakes> [Last accessed on 2023 Jun 10].
- Vamvatsikos, D., and Cornell, C.A., 2002. Incremental dynamic analysis. *Earthquake Engineering and Structural Dynamics*, 31, pp. 491-514.
- Vamvatsikos, D., and Cornell, C.A., 2004. Applied incremental dynamic analysis. *Earthquake Spectra*, 20, pp. 523-553.
- Vamvatsikos, D., and Fragiadakis, M., 2010. Incremental dynamic analysis for estimating seismic performance sensitivity and uncertainty. *Earthquake Engineering and Structural Dynamics*, 39, pp. 141-163.
- Vona, M., 2014. Fragility curves of existing RC buildings based on specific structural performance levels. *Open Journal of Civil Engineering*, 4, 120.
- Wang, Y., and Rosowsky, D.V., 2014. Effects of earthquake ground motion selection and scaling method on performance-based engineering of wood-frame structures. *Journal of Structural Engineering*, 142(10), pp. 04014086-1-11.
- Xue, Q., Wu, C.W., Chen, C.C., and Chen, K.C., 2008. The draft code for performance-based seismic design of buildings in Taiwan. *Engineering Structures*, 30, 1535-1547.